Evaluation of Reanalyzed Precipitation Variability and Trends Using the Gridded Gauge-Based Analysis over the CONUS

WENJUN CUI AND XIQUAN DONG

Department of Hydrology and Atmospheric Sciences, The University of Arizona, Tucson, Arizona

BAIKE XI AND AARON KENNEDY

Department of Atmospheric Sciences, University of North Dakota, Grand Forks, North Dakota

ABSTRACT

Atmospheric reanalyses have been used in many studies to investigate the variabilities and trends of precipitation because of their global coverage and long record; however, their results must be properly analyzed and their uncertainties must be understood. In this study, precipitation estimates from five global reanalyses [ERA-Interim; MERRA, version 2 (MERRA2); JRA-55; CFSR; and 20CR, version 2c (20CRv2c)] and one regional reanalysis (NARR) are compared against the CPC Unified Gauge-Based Analysis (CPCUGA) and GPCP over the contiguous United States (CONUS) during the period 1980–2013. Reanalyses capture the variability of the precipitation distribution over the CONUS as observed in CPCUGA and GPCP, but large regional and seasonal differences exist. Compared with CPCUGA, global reanalyses generally overestimate the precipitation over the western part of the country throughout the year and over the northeastern CONUS during the fall and winter seasons. These issues may be associated with the difficulties models have in accurately simulating precipitation over complex terrain and during snowfall events. Furthermore, systematic errors found in five global reanalyses suggest that their physical processes in modeling precipitation need to be improved. Even though negative biases exist in NARR, its spatial variability is similar to both CPCUGA and GPCP; this is anticipated because it assimilates observed precipitation, unlike the global reanalyses. Based on CPCUGA, there is an average decreasing trend of $-1.38 \, \text{mm yr}^{-1}$ over the CONUS, which varies depending on the region with only the north-central to northeastern parts of the country having positive trends. Although all reanalyses exhibit similar interannual variation as observed in CPCUGA, their estimated precipitation trends, both linear and spatial trends, are distinct from CPCUGA.

1. Introduction

Precipitation is a critical component of land surface processes and the hydrological cycle. It is also an important factor in understanding climate variability. Changing rainfall patterns have a significant impact on water sources and directly influence industrial and agricultural output as well as people's daily lives. The characteristics of precipitation over the contiguous United States (CONUS) differ significantly in time and space, which is the result of the interaction of several complex atmospheric and oceanic processes evolving at different spatial and temporal scales. To better understand the long-term rainfall variability and trends over the CONUS, an accurate and temporally and spatially homogenous precipitation dataset should be used.

Because of their spatial and temporal continuity, atmospheric reanalysis datasets have been widely used in climate research. Reanalyses are generated through a consistent data assimilation system and model, which incorporates observations and a background model forecast to generate uniform gridded data (Bosilovich et al. 2008). With continuous improvements in data assimilation methods and numerical models and the increasing availability of observational data from satellite and in situ measurements, recently developed reanalysis datasets can produce increasingly accurate output of atmospheric and oceanic variables for climate studies. However, errors and uncertainties can still be raised from aspects such as poor data quality, deficiency in

Corresponding author: Professor Xiquan Dong, xdong@email.arizona.edu

model physical parameterizations, and inhomogeneities introduced by changes in the observing system.

Global reanalyses do not directly generate precipitation analysis. In other words, precipitation is not a control variable in the analysis procedure, and thus precipitation in reanalysis is directly related to the physical parameterizations in the modeling system (Rienecker et al. 2011). For instance, Rienecker et al. (2011) concluded that even though microwave-retrieved rain rates are assimilated into models over oceans, humidity information derived from passive microwave measurements was found to have a much larger impact on the reanalyzed precipitation than precipitation observations themselves in the Modern-Era Retrospective Analysis for Research and Applications (MERRA). Therefore, errors may occur when models cannot simulate the physical mechanisms responsible for precipitation. In addition, precipitation in reanalysis products is influenced by changes in observational data, including the coverage and continuity of observation stations, radiosondes, and satellite instruments, which can lead to abrupt changes in precipitation records (Rienecker et al. 2011; Zhang et al. 2012). Hence, discontinuities introduced by changing observational systems may be found in reanalyzed climate data. To better understand and quantify the uncertainties in the precipitation estimates generated by reanalyses, comparisons with observation-based precipitation datasets should be performed.

To date, various studies regarding precipitation in reanalysis datasets have been performed, from regional to global spatial scales and from event to climate temporal scales (Ma et al. 2009; Wang and Zeng 2012; Bosilovich 2013; Lee and Biasutti 2014; Blacutt et al. 2015; Prakash et al. 2015; Dolinar et al. 2016). Bosilovich et al. (2008) evaluated global precipitation from five reanalyses using the Climate Prediction Center (CPC) Merged Analysis of Precipitation (CMAP) during the period 1979–2005. Results showed that the Japanese 25-year Reanalysis Project (JRA-25) performed better than the other four reanalyses in both the Northern Hemisphere continents and tropical oceans, but contained distinct variation depending on the available observing system. Kishore et al. (2016) validated four reanalyses with gridded India Meteorological Department (IMD) rainfall datasets over the Indian subcontinent and concluded that all reanalyses captured the strong interannual variations within the Indian region well, and of all the reanalyses, ERA-Interim showed the most realistic values with respect to IMD observations. Ashouri et al. (2016) evaluated the skill of MERRA in reproducing historical extreme precipitation events in the United States with CPC Unified Gauge-Based Analysis

(CPCUGA) data and showed that MERRA reasonably mimics the continental-scale patterns of change as observed by CPCUGA data while underestimating the magnitudes of extreme events, particularly over the Gulf Coast regions. These evaluation studies suggest that reanalyzed precipitation data differ seasonally and regionally, often with observations, despite the reanalysis precipitation products showing similar large-scale patterns to the observed precipitation.

In addition to reanalysis products, spatially and temporally uniform global precipitation datasets can also be generated by merging rain gauge observations with satellite analysis. These long-term, observation-based global precipitation products are favored in various research uses, including global climate change analysis, hydrological cycle studies, and verification of numerical models (Adler et al. 2003; Xie et al. 2003; Huffman et al. 2009). One such product is the Global Precipitation Climatology Project (GPCP) satellite–gauge (SG) combined product. GPCP produces monthly precipitation estimates by combining precipitation information available from each source into a final merged product, taking advantage of the strengths of each data type and removing biases based on hierarchical relations in the stepwise approach (Adler et al. 2003). The GPCP precipitation estimates have been used as reference data for many trend analyses and validation studies of climate models and reanalyses (Gu et al. 2007; Dee et al. 2011; Fensholt and Rasmussen 2011; Rienecker et al. 2011; Stanfield et al. 2015; Hatzianastassiou et al. 2016). With adequate satellite and Global Precipitation Climatology Centre (GPCC) gauge sampling over the CONUS, the estimates from GPCP might be a suitable tool to investigate the long-term pattern of precipitation over the United States. However, GPCP precipitation does have uncertainties associated with subjective (precipitation estimation and merging algorithms, input data processing) and objective factors (satellite instruments, rain gauge coverage), and these uncertainties should be taken into consideration when comparing GPCP with reanalyses.

Since the analysis in this study is conducted over the CONUS, the dense rain gauge networks should be taken advantage of. Therefore, a gridded gauge-based precipitation product is also included in this study to address the uncertainties in GPCP and validate the reanalyzed precipitation. Here, CPCUGA is employed. The creation of daily precipitation analysis in CPCUGA is done by interpolating gauge observations using objective analysis technique at fine spatial resolution. Chen et al. (2008a) evaluated three objective techniques to

determine the best one to be applied to CPC to obtain the gauge-based daily precipitation analysis. While all of the objective analysis techniques examined by Chen et al. (2008a) are adequate, optimal interpolation (OI) performed the best and is currently used in CPCUGA.

In this study, precipitation estimates from five global reanalyses, including ERA-Interim; MERRA, version 2 (MERRA2); Japanese 55-year Reanalysis (JRA-55); Climate Forecast System Reanalysis (CFSR); and Twentieth Century Reanalysis, version 2c (20CRv2c), as well as one regional reanalysis, North American Regional Reanalysis (NARR), are evaluated using the CPCUGA monthly analysis and GPCP, version 2.2, monthly products over the CONUS during the period from 1980 through 2013. Because CPCUGA is only available over global land, it is important to characterize GPCP for global use. Several global reanalyses used in this study assimilate satellite radiances to generate precipitation estimates therefore some data overlap occurs between them and GPCP. The comparisons with CPCUGA may identify if the biases in reanalyses originate from model parameterizations or the assimilated data. For instance, if both GPCP and reanalyses show similar bias patterns with respect to CPCUGA, it is most likely that the biases in reanalyses are originated from assimilated satellite radiances because GPCP also uses satellite-retrieved precipitation estimates from infrared (IR) and microwave measurements; otherwise, the biases are likely a result of the model parameterizations. Furthermore, the intercomparisons between global and regional reanalyses may reveal how assimilated data (with or without observed precipitation data) influence the precipitation output (e.g., NARR directly assimilates observed precipitation, unlike the global reanalyses). A trend analysis is also conducted to determine if reanalyses can be used in trend studies. The aim of this paper is to understand the characteristics of precipitation over the CONUS in the past three decades, to identify the uncertainties and errors associated with reanalyzed precipitation products, and to determine what improvements are needed, leading to better use in the future. It should be noted that the assessment in this paper may not be easily extendable to other regions because there are more datasets available from both satellites (better coverage) and radiosondes over the CONUS, which cannot be found over other regions.

2. Datasets

a. CPC Unified Gauge-Based Analysis Data

CPC Unified Gauge-Based Analysis data are produced as a part of the National Oceanic and Atmospheric Administration's (NOAA) CPC Unified Precipitation Project. This project aims to construct consistent and high-quality precipitation products over land globally (Chen et al. 2008a). The gauge analysis used in this study covers the CONUS at a fine spatial resolution of $0.25° \times 0.25°$ and is quantitatively consistent with that covering the global land on a coarser resolution of $0.5° \times 0.5°$ (Chen et al. 2008a). The daily precipitation is created based on quality-controlled daily gauge reports collected from NOAA/National Climatic Data Center (NCDC) River Forecast Centers (RFCs) and daily accumulations from Hourly Precipitation Data (HPD) set over the CONUS, which are then interpolated through the OI technique with an orographic effects correction (Xie et al. 2007). Based on a global gauge density plot from Chen et al. (2008b), there are more than three gauges within each $1° \times 1°$ grid box over the central and eastern parts of the CONUS and West Coast. However, gauge coverage is sparse over the mountainous regions, and some grid boxes over Montana and between California and Nevada have no gauges. The sparse coverage of gauge instruments can lead to significant sampling errors over these regions and underestimation by CPC precipitation analyses. These issues will be discussed further in section 5. Further details on the interpolation algorithm, gauge algorithm evaluation, and the construction of the dataset can be found in Xie et al. (2007) and Chen et al. (2008a, b). In this study, the gridded monthly CPC gauge analysis is used as the primary validation data to evaluate the performances of reanalyses.

b. GPCP SG combined (version 2.2) dataset

The GPCP product is produced at the National Aeronautics and Space Administration (NASA) Goddard Space Flight Center (GSFC). It provides global monthly precipitation estimates on a $2.5° \times 2.5°$ (longitude) grid from combined multisatellite and gauge observations and is available from January 1979 to present (Adler et al. 2003). For the satellite field, during the pre–Special Sensor Microwave Imager (SSM/I) period (1979–86), the estimates are based on the Outgoing Longwave Radiative (OLR) Precipitation Index (OPI) technique that retrieves precipitation using IR observations from low-Earth-orbiting satellites (Xie and Arkin 1998). After multiple meteorological satellites were launched in 1986, the SSM/I and Special Sensor Microwave Imager/Sounder (SSMIS; from 2008 to present) estimates calculated from the Wilheit et al. (1991) emission and Grody (1991) scattering algorithms; Television and Infrared Observation Satellite (TIROS) Operational Vertical Sounder (TOVS) and Atmospheric Infrared Sounder (AIRS) estimates based on the

TABLE 1. Summary of the reanalysis datasets used in this study. In the third column, 3DVAR stands for three-dimensional variational data assimilation and 4DVAR stands for four-dimensional variational data assimilation.

Reanalysis	Model resolution	Assimilation method	Horizontal grid spacing (lat × lon)	Temporal range	Reference
ERA-Interim	T255 L60	4DVAR	0.75° × 0.75°	From Jan 1979 to present	Dee et al. (2011)
MERRA2	72 sigma level	3DVAR	0.625° × 0.5°	From Jan 1980 to present	Rienecker et al. (2011); Bosilovich et al. (2015)
JRA-55	T319 L60	4DVAR	1.25° × 1.25°	From Jan 1958 to Dec 2013	Kobayashi et al. (2015)
CFSR	T382 L64	3DVAR	0.5° × 0.5°	From Jan 1979 to present	Saha et al. (2010)
20CRv2c	T62 L28	Ensemble Kalman filter	2° × 2°	From Jan 1851 to Dec 2014	Compo et al. (2011)
NARR	32 km	3DVAR	32 km × 32 km	From Jan 1979 to present	Mesinger et al. (2006)

methods of Susskind and Pfaendtner (1989) and Susskind et al. (1997); and the Geostationary Operational Environmental Satellite (GOES) precipitation index (GPI; Arkin and Meisner 1987) product have been added to the GPCP product. The GPI values are merged with SSM/I (SSMIS) estimates between 40°S and 40°N and calibrated by TOVS (AIRS) data at the 40° latitude bands to soften the transition poleward. Polarward from 40°, SSM/I (SSM/I)/TOVS (AIRS) data are used. The preliminary satellite field from both pre-SSM/I and SSM/I periods is climatologically calibrated with the gauge data from GPCC over the large-scale domain. Then, the gauge-adjusted satellite precipitation estimates are merged with GPCC gauge analyses for each grid box using the inverse variance weighting method to form the final SG monthly product. A more detailed description of input datasets and merging methods used in the GPCP product can be found in Adler et al. (2003), Huffman et al. (2009), and Huffman and Bolvin (2013).

c. Reanalysis datasets

In this study, the simulated monthly precipitation from five global reanalyses (ERA-Interim, MERRA2, JRA-55, CFSR, and 20CRv2c) and one regional reanalysis (NARR) are compared and evaluated with CPCUGA and GPCP products during the period from 1980 to 2013 over the CONUS. A general summary of each reanalysis dataset, including horizontal and spatial resolutions, temporal ranges, assimilation types, and references, is shown in Table 1.

1) ERA-INTERIM

ERA-Interim was developed by the ECMWF as a replacement for its preceding version, ERA-40 (Dee et al. 2011). Assimilated rain-affected SSM/I (SSMIS) radiances data from the Defense Meteorological Satellite Program (DMSP) series satellites as well as data from radiosonde and ground-based measurements are used as important input to generate a humidity analysis field. Compared to ERA-40, the revised humidity analysis scheme and method for minimizing biases in

radiance data have helped ERA-Interim produce more reasonable precipitation estimates with respect to observational-based precipitation product (Dee et al. 2011). The Sundqvist (1978) scheme is employed for large-scale precipitation simulation and the Lopez and Moreau (2005) scheme is adopted for convection parameterization.

2) MERRA2

MERRA2 is a NASA atmospheric reanalysis using a recent version of the Goddard Earth Observing System, version 5 (GEOS-5), data assimilation system (DAS; Bosilovich et al. 2015). MERRA2 uses an incremental analysis update that minimizes the spindown effects of the water vapor analysis. Although MERRA2 assimilates rain rate from SSM/I and Tropical Rainfall Measuring Mission (TRMM) Microwave Imager (TMI) over the ocean, these data are given a low weight and have a weaker impact on the increments than the humidity information derived from satellite radiance data [a full list of satellite radiance data assimilated into MERRA2 can be found in Koster et al. (2016)], as mentioned in the previous section. Over land, MERRA2 does not assimilate precipitation (Rienecker et al. 2011); therefore, it is similar to ERA-Interim, which produces a water vapor analysis field using in situ and satellite radiance data. Large-scale precipitation is simulated based on the scheme of Zhao and Carr (1997), which is sensitive to the moisture and cloud condensation over land (Rienecker et al. 2008). Convection is parameterized using the relaxed Arakawa–Schubert (RAS) scheme of Moorthi and Suarez (1992; Molod et al. 2015).

3) JRA-55

JRA-55 is the second Japanese global atmospheric reanalysis created by the Japan Meteorological Agency (JMA), which was first produced by the TL319 version of JMA's operational data assimilation system in December 2009. The newly available observations as well as the improved previous observations have helped JRA-55 produce considerably better simulated results

than JRA-25 (Kobayashi et al. 2015). To generate convection, a prognostic mass-flux-type Arakawa–Schubert scheme (Arakawa and Schubert 1974) with a convection-triggering mechanism known as the dynamic CAPE (DCAPE) generation rate from Xie and Zhang (2000) is adopted for the cumulus parameterization. The vertical profile of upward mass flux is assumed to be linear with height (Moorthi and Suarez 1992) and the mass flux at the cloud base is determined by solving a prognostic equation (Randall and Pan 1993). The scheme was updated by Nakagawa and Shimpo (2004) by considering the effect of detrainment due to downdrafts instead of simply reevaporating the precipitation, which cools and moistens the lower troposphere and represents convective downdrafts more realistically (Onogi et al. 2007).

4) CFSR

CFSR is produced by the National Centers for Environmental Prediction (NCEP). It contains various upgrades in model physics and assimilation algorithms compared to the previous NCEP reanalyses. Differing from other reanalysis datasets using only an atmospheric model, CFSR coupled the new GFS atmospheric model with Modular Ocean Model, version 4 (MOM4), to assimilate and predict atmospheric states every 6 h. For the atmospheric forecast model, a simplified Arakawa–Schubert scheme (Arakawa and Schubert 1974; Pan and Wu 1995; Hong and Pan 1998) is applied for the cumulus convection parameterization, with cumulus momentum mixing and orographic gravity wave drag (Kim and Arakawa 1995; Alpert et al. 1988). The shallow convection parameterization follows Tiedtke (1983) for wherever deep convection parameterization is not active.

5) 20CRV2C

The 20CR project is an effort led by NOAA and the University of Colorado Boulder's Cooperative Institute for Research in Environmental Sciences (CIRES) to produce a reanalysis dataset spanning the entire twentieth century, assimilating only surface observations of subdaily sea level pressure (SLP), monthly sea surface temperature (SST), and sea ice distributions as boundary conditions. Using the ensemble Kalman filter data assimilation approach (Whitaker and Hamill 2002), 20CRv2c directly yields each 6-h analysis as the most likely state of the global atmosphere and provides uncertainty estimates in the form of 56 realizations (Compo et al. 2011). 20CRv2c uses the same model as the NCEP Global Forecast System (GFS) 2008 experimental version (2008ex), version 2. By applying a prognostic cloud condensate scheme, the precipitation rate is parameterized following the approaches of Zhao and Carr (1997) for ice and Sundqvist et al. (1989) for liquid water.

6) NARR

NCEP NARR is a regional reanalysis that produces high-resolution analyzed atmospheric variables for the North American domain (Mesinger et al. 2006). NARR takes advantage of the recently operational version of the NCEP regional Eta model, where the convective parameterization is adopted from Betts–Miller–Janjić methods (Betts 1986; Janjić 1995). Unlike the global reanalyses, NARR does assimilate observed precipitation data as its latent heat profiles (Mesinger et al. 2006). Therefore, the precipitation field is not a product of just physical parameterizations (Bukovsky and Karoly 2007). Over the CONUS, the observed precipitation amounts from NCDC daily cooperative stations, RFC stations, and daily accumulations of HPD are analyzed using an inverse-square-distance weighting scheme and an orographic enhancement technique (Daly et al. 1994) to obtain a ⅛° daily analysis, then the daily CONUS analysis is disaggregated to an hourly analysis using temporal weights derived from a 2.5° analysis of hourly rain gauge data (Mesinger et al. 2006).

3. Methodology

Two reference datasets and six reanalyses are regridded to 2° × 2° to match the spatial resolution of 20CRv2c. All comparisons and trend analyses are conducted based on the grid box of 2° × 2° with a total of 260 grid boxes over the study domain. Because precipitation patterns over the CONUS vary in space and time, the study domain is divided into six subdomains: West Coast (WC), Mountain West (MW), Northern Great Plains (NGP), Northeast (NE), Southern Great Plains (SGP), and Southeast (SE), as shown in Fig. 1a. Comparisons are performed for four seasons: spring (MAM), summer (JJA), fall (SON), and winter (DJF). Several statistical metrics, such as correlation coefficient, root-mean-square error (RMSE), and relative difference percentage (RDP) are calculated to evaluate the performance of reanalysis precipitation based on their computed domain and subdomain monthly mean precipitation. The RDP is defined as

$$\text{RDP} = (R - \text{CPCUGA})/\text{CPCUGA} \times 100\%, \quad (1)$$

where R represents the precipitation amounts from the GPCP and reanalyses. Spatial distributions of annual and seasonal precipitation, as well as the correlation coefficients between reanalyses and CPCUGA, are also plotted, with significant tests performed for each grid box. Additionally, to investigate the differences between CPCUGA and the reanalyses in precipitation distribution, probability density functions (PDFs) and
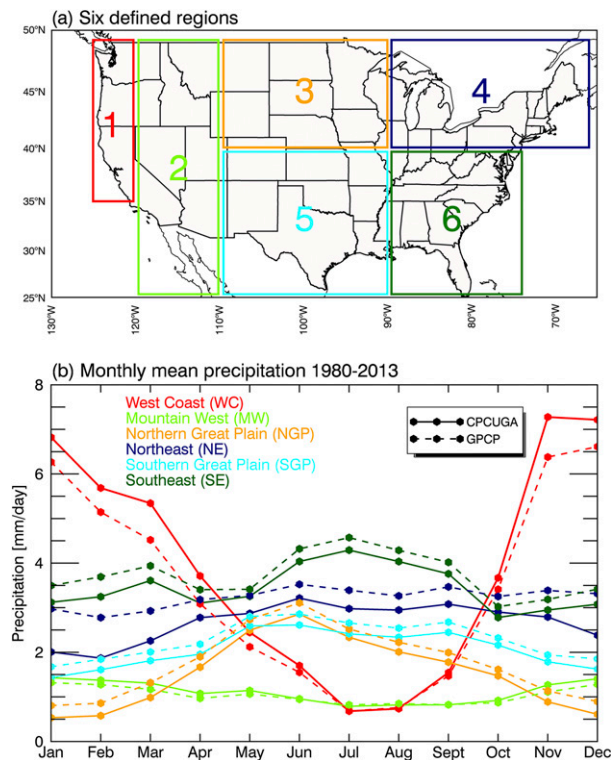
FIG. 1. (a) CONUS divided into six regions: 1) WC, 2) MW, 3) NGP, 4) NE, 5) SGP, and 6) SE. (b) Monthly mean precipitation of CPCUGA (solid) and GPCP (dashed) for each region during the period 1980–2013.

FIG. 2. Scatterplot of monthly mean precipitation between CPCUGA and GPCP. There are a total of 106 080 (260 grid boxes × 408 months) points on the plot. The color bar indicates the number density.

cumulative distribution functions (CDFs) are computed from all monthly precipitation estimates. In terms of trend analysis, a linear regression function is applied to annual accumulated precipitation from two reference datasets and six reanalyses. Their interannual trends are generated by minimizing the chi-squared error, and the trend spatial distributions of monthly precipitation anomaly during a 34-yr study period are plotted to demonstrate the regional differences in precipitation trend over the CONUS. Nonparametric Mann–Kendall tests (Mann 1945; Kendall 1975) are applied to each grid box to examine if the trends are significant at the 95% confidence level.

4. Results

a. Comparison between CPCUGA and GPCP

To quantitatively assess GPCP, a simple comparison with CPCUGA is performed. The monthly mean precipitation from two datasets during the study period for each subdomain is shown in Fig. 1b. Except for the NE region, where GPCP shows less seasonal variability compared to CPCUGA, the monthly precipitation

pattern agrees well between two datasets for the five subdomains. In terms of precipitation amount, GPCP is higher than CPCUGA, except for the MW and WC regions. The differences between the two datasets are around 1 mm day^{-1} during the winter months over the NE region. Figure 2 is the scatterplot of monthly precipitation for each 2° grid box. There are a total of 106 080 (260 grid boxes × 408 months) paired points during the 34-yr period. The two datasets show a strong linear relationship and are well correlated with each other; however, the mean precipitation estimated by GPCP is ~8% higher than CPCUGA. Also, if treating CPCUGA precipitation values as "truth," GPCP has an RMSE of 0.75 mm day^{-1}. The comparisons in Figs. 1 and 2 have suggested that GPCP may have a wet bias, particularly over the Great Plains and East Coast, but overall performs well when compared with CPCUGA.

b. Evaluation of reanalyzed precipitation

Figure 3 illustrates the spatial distribution of annual mean precipitation of CPCUGA, GPCP, and the six reanalyses over the CONUS during the period 1980–2013. Figures 3a and 3b show that the observed precipitation amounts generally decrease from the East Coast to the West Coast, with the highest rainfall amounts over the northwest coast, southeast coast, and south-central parts of the United States, while the lowest amounts occur over the mountainous regions. The reanalyses demonstrate reasonable spatial distributions with respect to the CPCUGA and GPCP results and capture the variation of the precipitation climate regime very well, particularly over the Pacific Northwest region.
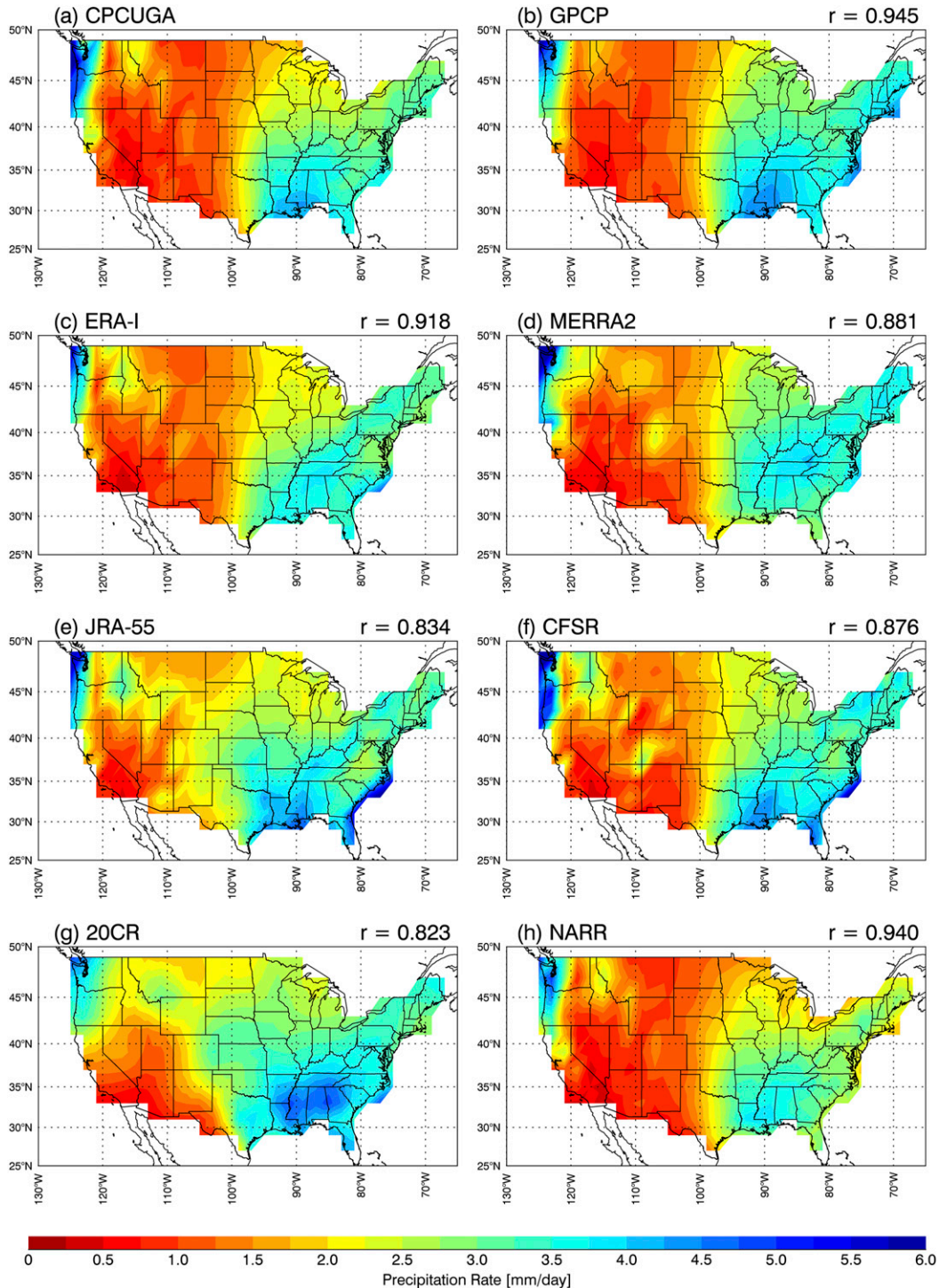
FIG. 3. Spatial distribution of annual mean precipitation (mm day^{-1}) for (a) CPCUGA, (b) GPCP, and (c)–(h) the six reanalyses during the period 1980–2013. Also shown are the pattern correlation r values between CPCUGA and GPCP and between CPCUGA and reanalyses.

However, large differences exist between the two reference datasets and the global reanalyses over the mountainous areas where precipitation amounts simulated by the global reanalyses are generally higher than both CPCUGA and GPCP. Most of the observed precipitation amounts range from 0.25 to 1.75 mm day^{-1}, while

precipitation from all five global reanalyses can exceed 2.5 mm day^{-1} over the mountainous regions. 20CRv2c and JRA-55 also have large areas with discontinuities in precipitation distribution located over southern Montana. NARR exhibits a very similar pattern as the two reference datasets, but precipitation amounts estimated by NARR are less intense over the eastern CONUS. The spatial patterns of reanalyzed annual mean precipitation are all well correlated with CPCUGA, ranging from 0.823 in 20CRv2c to 0.940 in NARR.

Figure 4a shows CPCUGA's averaged seasonal mean precipitation (spring, summer, fall, and winter) during the study period. Except for the western mountainous regions, which receive the least precipitation throughout the year, the precipitation distributions show significant seasonal variations over the CONUS based on the CPCUGA data. Figures 4b–h show the differences of seasonal mean precipitation (%) between CPCUGA and GPCP, and six reanalyses. The gray crosses represent the grid points having RDP values outside of the two standard deviations.

The GPCP precipitation amounts are more than CPCUGA, except for the northwest and certain parts of mountainous regions throughout the year. Large differences also exist between the global reanalyses and CPCUGA for roughly the same areas. The seasonal spatial distributions of ERA-Interim, MERRA2, and CFSR are similar to each other in that they underestimate the precipitation amounts over the south-central regions during spring, fall, and winter and over the Great Plains during summer. The RDP patterns in JRA-55 during fall and winter are similar to the three reanalysis datasets mentioned above, but during summer overestimation is found in JRA-55 over the Great Plains. With regard to 20CRv2c, there is a negative bias in the West Coast for all seasons and significant underestimation over the southwest during summer. Differing from the other reanalyses, 20CRv2c severely overestimates precipitation amounts over the mountainous and central regions during spring, summer, and winter. The distributions of NARR's RDPs are distinct from global reanalyses, with relative low spatial biases, between −10% and 10%, over the CONUS domain.

The seasonal mean precipitation amounts (mm day^{-1}) and their standard deviations estimated by CPCUGA, GPCP, and the six reanalyses are listed in Table 2. CPCUGA has an annual mean precipitation of 2.21 mm day^{-1} with a standard deviation of 2.00 mm day^{-1}. The seasonal mean precipitation of CPCUGA ranges from 2.02 mm day^{-1} during winter to 2.39 mm day^{-1} during summer; the same goes for GPCP, except the GPCP precipitation amounts are higher. The highest standard deviation of 2.24 mm day^{-1}

for CPCUGA occurs during winter and is likely because of the large precipitation amounts in the northwestern region that increase the variation of precipitation values. Table 3 provides the RDPs (%) and RMSEs (mm day^{-1}) of six reanalyses using CPCUGA as reference data, and using GPCP as reference data for seasonal mean precipitation in each defined region. Over the WC, the precipitation values are underestimated by ERA-Interim, JRA-55, 20CRv2c, and NARR year-round, and their RMSEs are high during the winter season when abundant precipitation falls in this region. Apart from NARR, which slightly underestimates precipitation, overestimation of ~20% is found in global reanalyses over the MW. Significant overestimation of winter season precipitation over the NGP and NE is also found in global reanalyses. The RDP values have less seasonal variation over the SE, probably due to the least variation of precipitation types associated with the subtropical climate over this region. NARR underestimates the precipitation year-round in all regions, though the overall biases and RMSE values compared with CPCUGA and GPCP are the smallest among all six reanalyses. For global reanalyses, ERA-Interim and MERRA2 show better performance in terms of the relatively lower RMSE values. It is noted that most RMSEs calculated using GPCP as reference are smaller than those using CPCUGA as reference in four reanalyses that assimilate satellite radiances, which makes sense because GPCP uses satellite-retrieved precipitation.

Correlation coefficients of monthly precipitation between CPCUGA and GPCP and between CPCUGA and reanalyses were calculated for each grid box and are shown in Fig. 5. Grid points that are significant at the 95% confidence interval based on a one-tailed z test using the Fisher r-to-z transformation (Fisher 1915) are also shown as gray crosses in Fig. 5. The spatial distributions of correlation coefficients have illustrated that NARR is in excellent agreement with CPCUGA, with correlation coefficients exceeding 0.95 over most of the CONUS. GPCP is less correlated with CPCUGA compared to NARR, but correlation coefficients are still greater than 0.9. The global reanalyses are strongly correlated with CPCUGA over the U.S. West Coast, where values are higher than 0.9. ERA-Interim and JRA-55 have significantly high correlations over the north-central to northeastern parts of the country, while MERRA2 is well correlated with CPCUGA over the north-central and southwestern regions. Correlations less than 0.7 over the northern to central mountainous regions in global reanalyses correspond to the regions where they underestimate precipitation as shown in Fig. 4. 20CRv2c is less correlated with CPCUGA with respect to other reanalyses. Lower correlations around
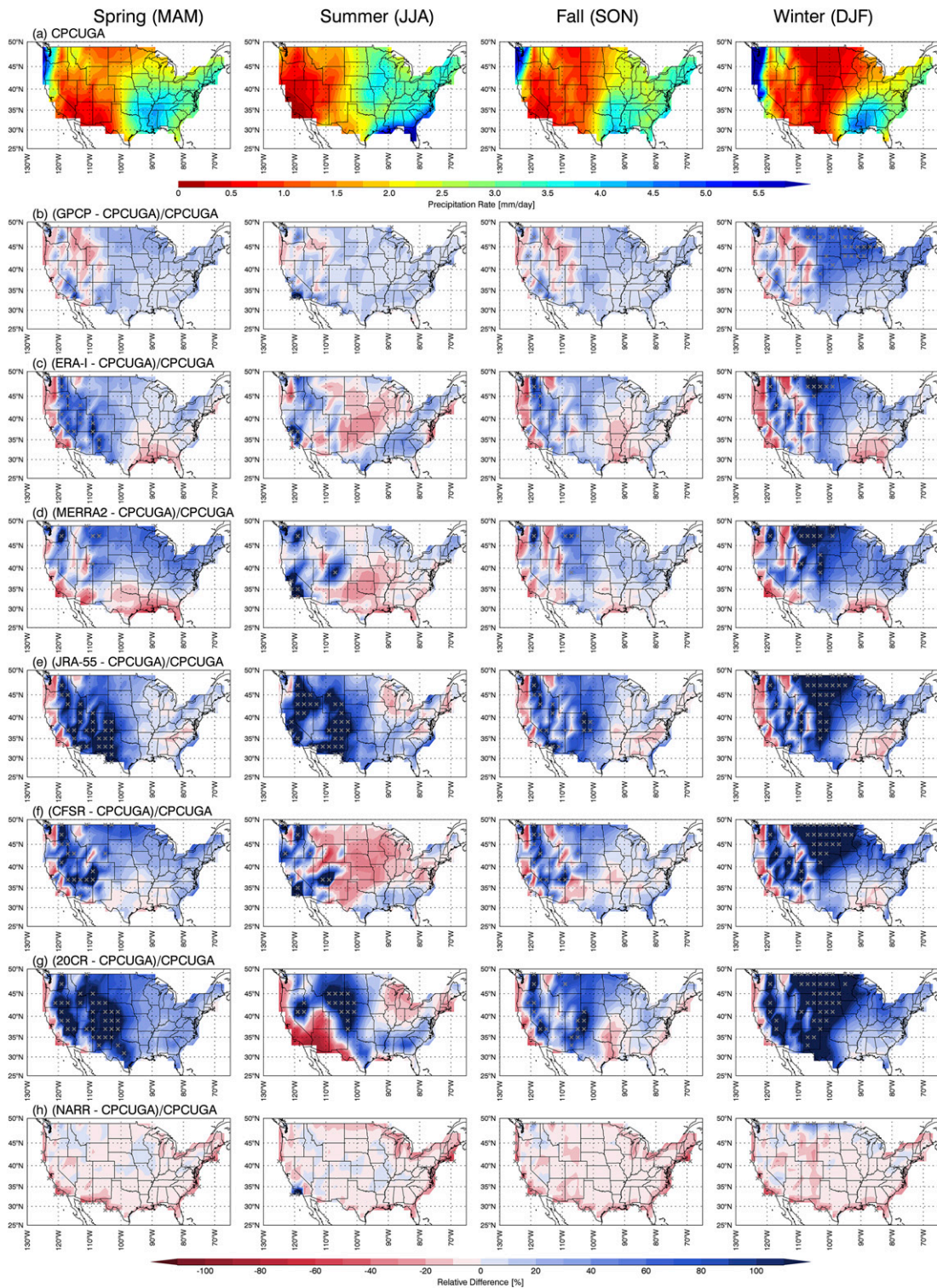
FIG. 4. Spatial distribution of (a) seasonal mean precipitation (mm day^{-1}) for CPCUGA and (b)–(h) seasonal RDP between CPCUGA and GPCP and between CPCUGA and the six reanalyses during the period 1980–2013. The gray crosses indicate the grid boxes having RDP values outside of the two std devs.

TABLE 2. Year-round and seasonal mean precipitation values (mm day^{-1}) and std dev (in parentheses) estimated by CPCUGA, GPCP, and the six reanalyses.

	Year-round	Spring (MAM)	Summer (JJA)	Fall (SON)	Winter (DJF)
CPCUGA	2.21 (2.00)	2.24 (1.80)	2.39 (1.88)	2.17 (2.05)	2.02 (2.24)
GPCP	2.39 (1.91)	2.39 (1.72)	2.58 (1.86)	2.32 (1.94)	2.27 (2.08)
ERA-Interim	2.24 (1.78)	2.34 (1.58)	2.45 (1.92)	2.17 (1.79)	1.99 (1.80)
MERRA2	2.36 (2.00)	2.55 (1.90)	2.36 (1.83)	2.29 (2.03)	2.25 (2.22)
JRA-55	2.66 (2.01)	2.74 (1.74)	3.13 (2.19)	2.47 (2.02)	2.29 (1.96)
CFSR	2.47 (2.10)	2.69 (1.87)	2.33 (2.21)	2.41 (2.20)	2.44 (2.11)
20CRv2c	2.73 (1.98)	3.15 (1.91)	2.75 (2.29)	2.38 (1.79)	2.65 (1.80)
NARR	1.97 (1.70)	2.05 (1.61)	2.15 (1.63)	1.88 (1.67)	1.79 (1.87)

0.2–0.35 are found between CPCUGA and 20CRv2c from eastern Arizona to western New Mexico.

Histograms of the PDFs and CDFs of monthly mean precipitation from CPCUGA (blue line), GPCP (red line), and the six reanalyses (red line) are plotted in Fig. 6 (a total of 260 grid boxes × 408 months). The median precipitation values of CPCUGA (blue), GPCP (red), and the reanalyses (red) are shown along the dashed lines in Fig. 6. GPCP has a higher median value than NARR (1.99 vs 1.74 mm day^{-1}), and some differences in frequency are found for precipitation with a range from 0–2 to 3–6 mm day^{-1}. Except NARR, all reanalyses have fewer precipitation estimates less than 1.0 mm day^{-1}, especially in JRA-55 and 20CRv2c. The percentages of JRA-55 and 20CRv2c precipitation amounts that are less than 1 mm day^{-1} are ~20%, which is ~10% less than the CPCUGA estimates—this is most likely due to their relatively coarse spatial resolution (2° × 2° for 20CRv2c and 1.25° × 1.25° for JRA-55). With coarser resolution, more precipitation likely comes from parameterized convection; therefore, they tend to generate fewer estimates with lower precipitation amounts. Their PDFs are skewed toward higher precipitation values (i.e., more skewed), especially 20CRv2c; thus, the median of 20CRv2c is much higher than CPCUGA (2.41 vs 1.74 mm day^{-1}). The precipitation distributions have relatively small differences between ERA-Interim, MERRA2, and CFSR, and they have more precipitation estimates between 1.0 and 6.0 mm day^{-1}. Unexpectedly, the total numbers of high precipitation days (>8.0 mm day^{-1}) from the five global reanalyses agree well with CPCUGA, presumably due to the small number of samples. As for NARR, its distribution is more skewed to the lower precipitation values, which results in a consistent low bias in NARR.

c. Trend analysis

Changes in the input data sources will lead to inhomogeneities in satellite-based GPCP and in reanalysis products that assimilate satellite observations, and could result in false trending. Zhang et al. (2012) summarized up to 12 major changes in observation systems in CFSR, such as the introduction of TOVS in 1979, the inclusion of Geostationary Meteorological Satellite (GMS) from JMA in 1987, and the incorporation of AIRS in 2004. Although GPCC gauge observations are merged into GPCP to form the final monthly precipitation product and precipitation estimates of GPCP are likely less sensitive to the changes of satellite observations, particularity over areas that have relatively dense GPCC coverage such as the CONUS, caution should still be taken when using it to study trends since it is still primarily based on satellite data. Therefore, to determine if GPCP and reanalyzed precipitation can be used for climatology trend studies, trend analyses are conducted here. Figure 7 shows the interannual variability of CPCUGA, GPCP, and reanalyzed annual accumulated precipitation over the CONUS during the 34-yr study period. The blue line represents the linear regression fit to the annual accumulated precipitation by minimizing the chi-squared error. The shaded areas contain the precipitation values within two standard deviations of the slope. CPCUGA annual accumulated precipitation and its calculated trend are illustrated as dashed lines in Figs. 7b–h CPCUGA has an annual average precipitation of 806.0 mm, while GPCP has an average of 873.1 mm with similar interannual variations during the 34-yr period. The annual accumulated precipitation maximum (940.7 mm for CPCUGA, 1002.3 mm for GPCP) occurred in 1983 while lows (772.2 and 734.2 mm for CPCUGA, 794.1 and 735.6 mm for GPCP) occurred in 1988 and 2012 in both CPCUGA and GPCP.- According to the regression line, CPCUGA and GPCP show negative trends of −1.38 and −1.83 mm yr^{-1}, respectively. In terms of reanalyses, although they exhibit similar interannual variability of precipitation to CPCUGA (dashed line), their precipitation amounts are significantly different. During the study period, MERRA2, JRA-55, 20CRv2c, and CFSR have consistent positive biases, while NARR has a consistent negative bias compared to CPCUGA. The annual accumulated precipitation in ERA-Interim is more than CPCUGA

TABLE 3. For each reanalysis, the RDP (%) compared with CPCUGA, the RMSE (mm day^{-1}) calculated using CPCUGA as reference data, and the RMSE (mm day^{-1}) calculated using GPCP as reference data is given for four different seasons over six defined regions in Fig. 1a. The boldface numbers represent the max and min RDPs in each region.

	WC				MW				NGP				NE				SGP				SE			
	MAM	JJA	SON	DJF	MAM	JJA	SON	DJF	MAM	JJA	SON	DJF	MAM	JJA	SON	DJF	MAM	JJA	SON	DJF	MAM	JJA	SON	DJF
ERA-Interim																								
RDP from CPCUGA (%)	−21.6	−2.9	−22.5	**−28.3**	33.7	13.8	15.3	3.3	18.7	−6.7	12.8	44.8	7.2	3.0	0.9	13.4	4.4	−0.4	2.1	5.9	−3.9	8.8	−1.1	−4.4
RMSE with CPCUGA (mm day^{-1})	1.55	0.58	2.08	2.81	0.89	0.67	0.79	1.03	0.74	1.02	0.63	0.40	0.82	1.15	0.89	0.68	1.10	1.29	1.09	0.78	1.18	1.57	1.27	1.12
RMSE with GPCP (mm day^{-1})	1.01	0.42	1.35	2.02	0.90	0.65	0.68	0.79	0.68	0.99	0.58	0.34	0.79	1.09	0.89	0.94	1.03	1.21	1.01	0.77	1.11	1.42	1.19	1.06
MERRA2																								
RDP from CPCUGA (%)	8.2	28.4	−5.1	2.2	9.7	11.7	0.2	0.7	43.4	4.9	25.1	78.9	40.0	11.3	9.7	28.3	−6.6	**−12.4**	2.0	9.3	3.2	−9.4	4.0	8.1
RMSE with CPCUGA (mm day^{-1})	1.73	0.85	2.10	2.81	0.69	0.54	0.67	0.96	1.11	1.28	0.78	0.57	1.46	1.37	1.09	0.91	1.25	1.40	1.21	0.90	1.60	1.62	1.45	1.38
RMSE with GPCP (mm day^{-1})	1.69	0.70	1.49	2.47	0.62	0.50	0.51	0.71	0.90	1.18	0.68	0.44	1.11	1.21	0.94	0.82	1.20	1.37	1.08	0.83	1.45	1.48	1.22	1.12
JRA-55																								
RDP from CPCUGA (%)	−16.6	13.7	−15.7	−19.2	54.1	**77.1**	35.4	20.7	38.9	34.2	36.3	94.9	10.1	−1.4	5.0	29.3	44.4	58.3	24.2	23.4	7.2	19.4	7.5	3.8
RMSE with CPCUGA (mm day^{-1})	1.64	0.68	2.13	2.11	1.22	1.17	0.98	1.81	1.08	1.53	0.87	0.67	0.83	1.15	0.92	0.88	1.56	2.12	1.32	0.97	1.21	1.88	1.52	1.09
RMSE with GPCP (mm day^{-1})	1.20	0.54	1.50	2.99	1.23	1.13	0.91	1.02	0.97	1.38	0.75	0.48	0.75	1.09	0.88	0.76	1.40	1.95	1.20	0.91	1.12	1.74	1.39	1.07

TABLE 3. (*Continued*)

|	WC				MW				NGP				NE				SGP				SE			
	MAM	JJA	SON	DJF	MAM	JJA	SON	DJF	MAM	JJA	SON	DJF	MAM	JJA	SON	DJF	MAM	JJA	SON	DJF	MAM	JJA	SON	DJF
CFSR																								
RDP from CPCUGA (%)	2.0	**38.0**	−5.5	−9.2	45.4	21.4	23.9	29.1	41.3	**−21.1**	23.0	125.0	29.7	−3.7		**43.5**	7.5	−4.1	6.6	18.6	12.4	3.7	13.5	10.3
RMSE with CPCUGA (mm day^{-1})	1.98	1.10	2.45	2.99	1.12	0.93	0.92	1.28	1.14	1.31	0.83	0.86	1.23	1.25	1.09	1.18	1.15	1.62	1.22	0.87	1.42	2.16	1.74	1.22
RMSE with GPCP (mm day^{-1})	1.88	1.01	1.92	2.53	1.14	0.90	0.87	1.17	0.97	1.36	0.74	0.62	0.95	1.23	0.98	0.81	1.14	1.63	1.18	0.83	1.30	2.14	1.60	1.09
20CRv2c																								
RDP from CPCUGA (%)	−7.5	−19.0	−14.3	−12.2	71.5	6.6	25.0	51.5	73.7	49.0	47.7	**156.8**	27.0	−11.1	7.9	39.3	**60.8**	18.5	8.2	49.1	**26.9**	12.9	1.5	17.5
RMSE with CPCUGA (mm day^{-1})	1.92	0.73	2.01	2.81	1.34	1.11	0.97	1.18	1.68	2.22	1.11	1.00	1.23	1.33	1.21	1.09	2.07	2.28	1.55	1.24	1.65	2.02	1.47	1.33
RMSE with GPCP (mm day^{-1})	1.08	0.52	1.12	1.51	1.40	1.11	0.97	1.18	1.52	2.08	0.97	0.78	0.97	1.35	1.09	0.85	1.87	2.18	1.46	1.10	1.43	1.78	1.38	1.14
NARR																								
RDP from CPCUGA (%)	−15.3	−14.5	−19.4	−16.6	−2.2	−3.8	−5.1	**−6.9**	−2.00	−6.0	−6.4	−0.9	−13.4	**−18.3**	**−18.3**	−9.00	−4.9	−5.1	−10.4	−9.5	−8.8	−12.6	**−14.3**	−11.4
RMSE with CPCUGA (mm day^{-1})	1.45	0.51	1.98	2.58	0.29	0.28	0.29	0.49	0.29	0.48	0.30	0.19	0.75	0.98	0.97	0.63	0.46	0.61	0.60	0.45	0.81	1.19	1.06	0.81
RMSE with GPCP (mm day^{-1})	0.79	0.35	1.25	1.60	0.45	0.35	0.43	0.61	0.52	0.64	0.50	0.45	1.09	1.21	1.29	1.37	0.64	0.75	0.78	0.67	0.98	1.25	1.14	1.04
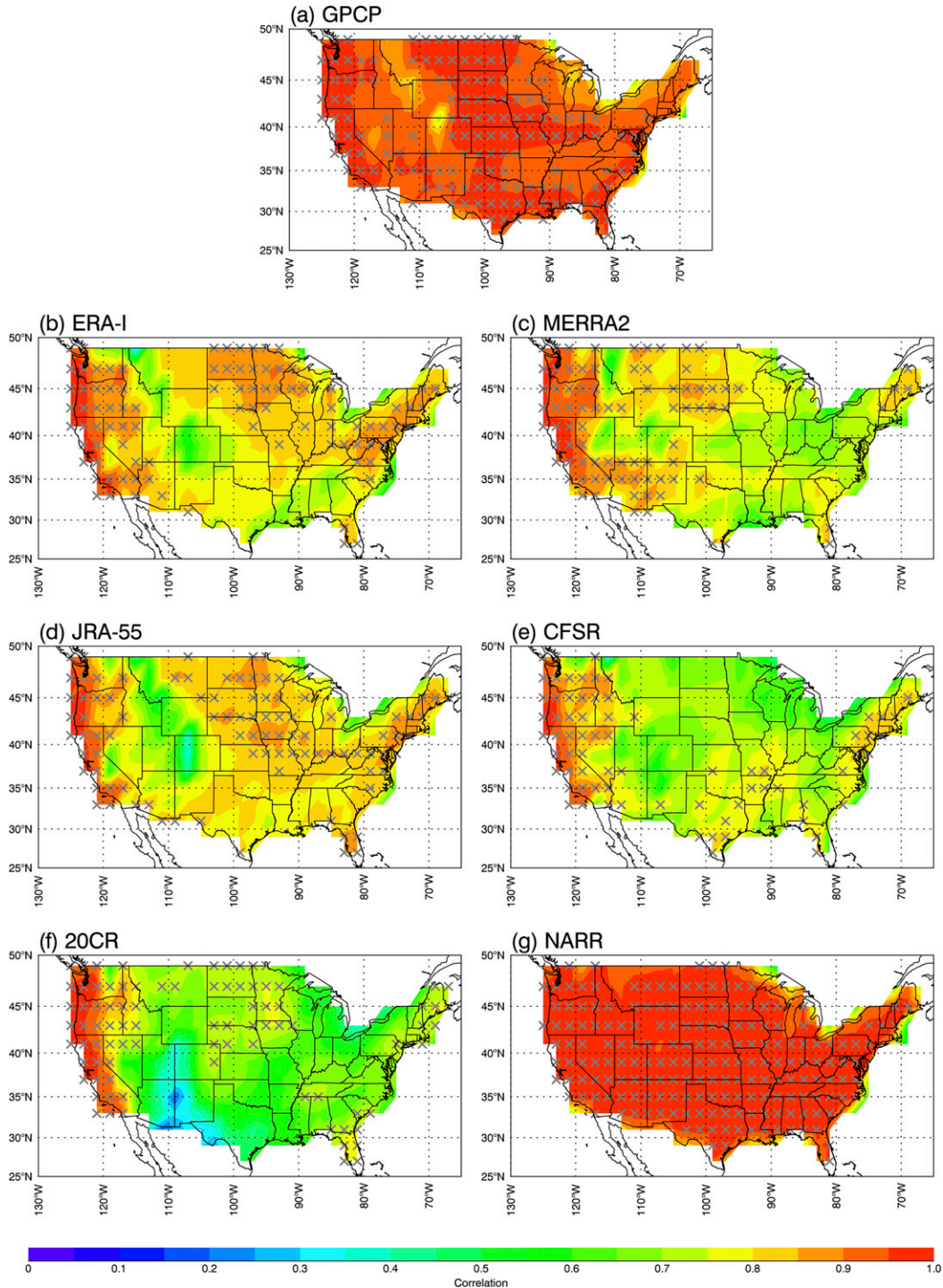
FIG. 5. Spatial distribution of correlation coefficients between CPCUGA and GPCP and between CPCUGA and the six reanalyses during the period 1980–2013. The gray crosses indicate the grid boxes with statistical significance at the 95% confidence level based on a one-tailed z test using the Fisher r-to-z transformation.

from 1980 through 1995, but their differences gradually decrease from 1996 to 2004 until ERA-Interim is below CPCUGA. This pattern leads to a significant decreasing

trend in ERA-Interim. Besides ERA-Interim, only JRA-55 ($-0.69 \, \mathrm{mm \, yr^{-1}}$) and 20CRv2c ($-0.33 \, \mathrm{mm \, yr^{-1}}$) generate negative trends, but their magnitudes are much
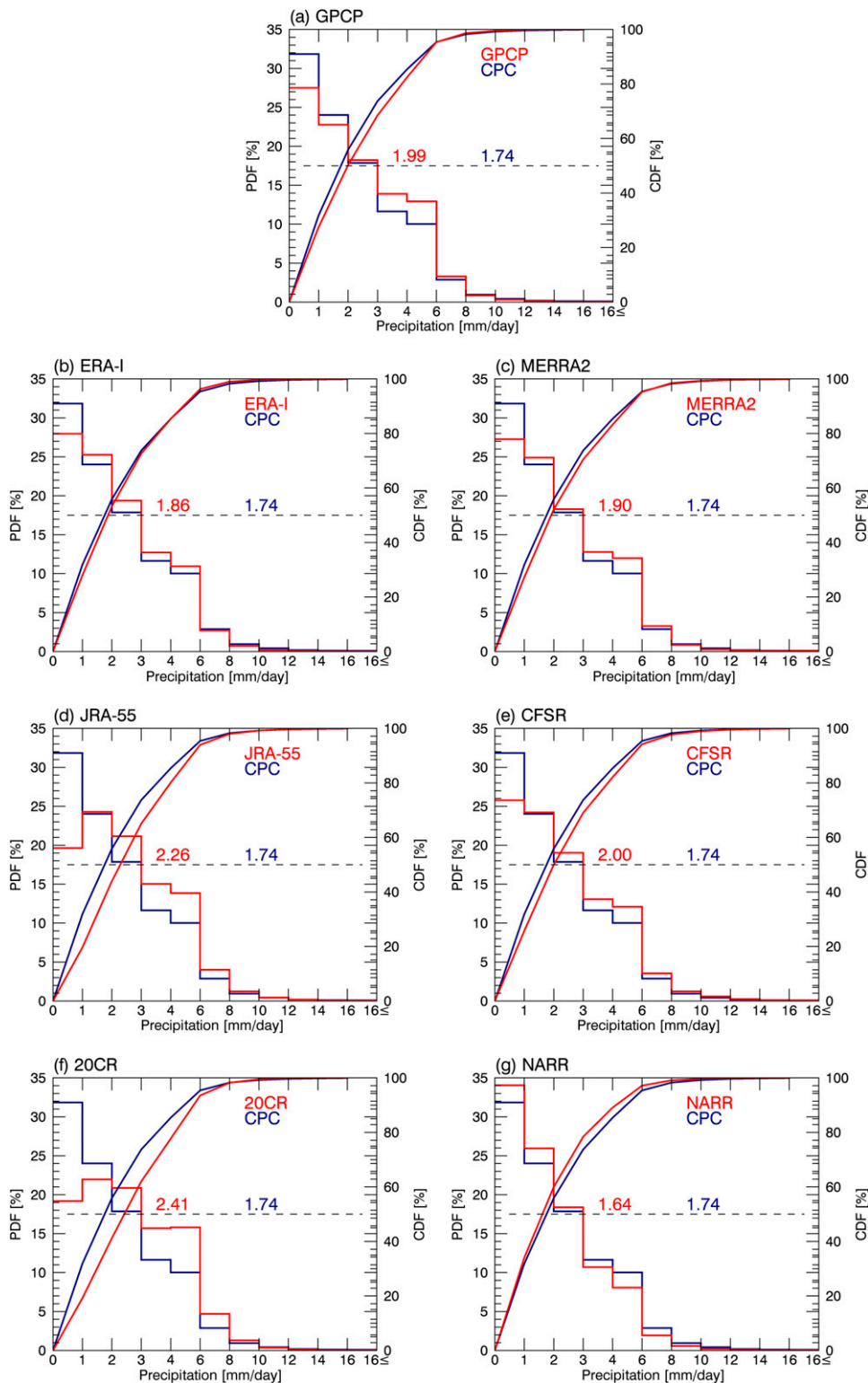
FIG. 6. PDFs (%) and CDFs (%) for CPCUGA (blue) and GPCP and the six reanalyses (red) of monthly mean precipitation (mm day^{-1}). Dashed lines represent the median line. The values listed in the plots are the median monthly mean precipitation of CPCUGA (blue) and the GPCP (red) and reanalyses (red).
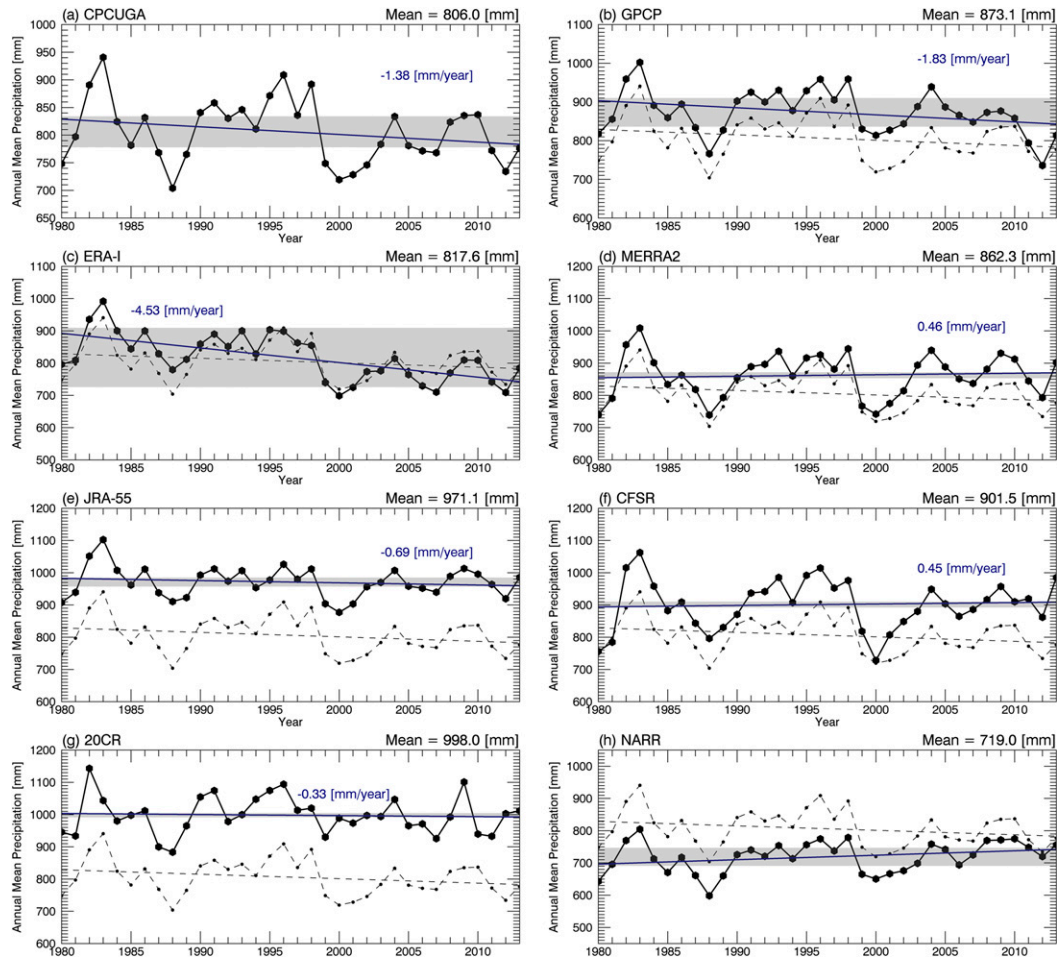
FIG. 7. (a)–(h) Linear trends (dark blue line) calculated from annual accumulated precipitation (mm; solid black circle and line) of CPCUGA, GPCP, and the six reanalyses during the period of 1980–2013. The shaded areas represent the area within 95% confidence interval of the slope based on the z test. The annual accumulated precipitation and linear trend of CPCUGA are also plotted as dashed lines in (b)–(h) as a baseline.

less than CPCUGA's trend. MERRA2 and CFSR have slightly increasing trends of 0.46 and 0.45 mm yr^{-1}, respectively. A positive trend is also found in NARR, with an increasing annual precipitation of 1.38 mm yr^{-1}, which is identical in magnitude to CPCUGA, but with an opposite sign.

Furthermore, in order to study the variation of regional precipitation trends, trend analysis of spatial distribution based on calculated monthly precipitation anomaly is also conducted. Based on the 34 years of data, the precipitation trend is calculated at each grid box using the same linear regression method as above. In addition, the Mann–Kendall test is used to determine if each grid box has an increasing or decreasing trend that is significant at the 95% confidence level. Grid boxes having trends with statistical significance at the 95% confidence interval are marked with gray crosses in Fig. 8. Based on CPCUGA and GPCP distributions,

the northeastern and north-central parts of the country have positive trends, while other regions have negative trends. Both increasing and decreasing trend rates are moderate in CPCUGA and GPCP, with a range from −0.3 to 0.3 mm yr^{-1} over most of the CONUS domain. In both datasets the negative trends are found over the central to southern mountainous regions. The spatial trend distributions of the reanalyses vary significantly. Of all six reanalyses, MERRA2 and CFSR show spatial distributions closest to the two reference datasets, but again, the magnitudes are different, such as the increasing trends being more intense (~0.6 mm yr^{-1}) in these two reanalyses over the north-central and northeastern regions. Significant decreasing trends can be up to −0.9 mm yr^{-1} in ERA-Interim over the majority of the CONUS, as seen in Fig. 8. Except for the central to mountainous western portions of the country, which have evident negative trends, positive trends are found

everywhere else in JRA-55. It seems assimilating gauge observations does not really help NARR to generate proper precipitation trends. The overall performance of the reanalyses in generating trends is unreliable.

5. Discussion

GPCP-derived precipitation values are generally higher than CPCUGA. This could be due to the issues associated with satellite precipitation estimates from GPCP. Satellite precipitation amounts are typically retrieved from cloud information such as the cloud-top temperature, cloud-top height, etc., while gauge observations only indicate how much precipitation has reached the ground. Therefore, overestimations may occur in satellite-based precipitation due to evaporation of precipitation before it reaches the ground. The combination of GPCC gauge observations and satellite measurements do help GPCP to generate more reliable precipitation trends over the CONUS; however, how they are weighted may influence the results. For example, in this study an overall wet bias is found in GPCP precipitation.

In terms of the reanalysis datasets, they illustrate reasonable spatial distributions of precipitation over the CONUS when compared with the two reference datasets, but significant seasonal and regional differences exist (Fig. 4). Over the mountainous regions, precipitation amounts simulated by global reanalyses are generally higher than CPCUGA (Table 3) throughout the year. The RDP patterns of the four reanalyses that assimilate satellite radiances are very similar to GPCP's. It could be problematic that the satellite retrievals, both IR and passive microwave, have difficulties detecting shallow, orographic precipitation (Adler et al. 2003). Issues that may also be associated with reanalyses over this region are the model difficulties in accurately estimating precipitation over complex terrain, as well as the lack of observational upper-air reports from meteorological stations assimilated into the models. Regarding GPCP, another possible reason to explain its performance over the mountainous region could be because the gauge reports from GPCC are less than those collected by CPC, leading to the underestimation over these areas for all seasons. The underestimation by GPCP over orography was also found in McPhee and Margulis (2005) and Nijssen et al. (2001) and is attributed to the sparse distribution of rain gauges in mountainous regions. Therefore, GPCP might not be suitable to use as a reference data for validation studies over complex terrain. Meanwhile, CPCUGA estimates may face the gauge undercatch issue. For example, over Montana and between California and Nevada, the

CPCUGA estimates are less than GPCP estimates throughout the year; these regions have sparse gauge density, as mentioned in section 2. Even though orographic effects are considered when applying the OI analysis, large uncertainties can still exist with fewer or without any gauge observations. For NARR, the differences between it and CPCUGA are much smaller over the mountainous terrain compared to GPCP. This could be because NARR assimilates the observed precipitation from the same gauge stations as in CPCUGA, and also applies an orographic enhancement technique. In addition to positive biases over mountainous regions, negative biases are found in the six reanalyses as well as in GPCP over the north-central and northeastern parts of the country, especially during winter when snowfall and sometimes heavier convective snowfall often occur. This issue may be associated with the uncertainties in satellite data over high latitudes during snow events. The overestimations in global reanalyses are more severe than in GPCP, indicating that the models used in the reanalyses may be less skillful in reproducing snowfall events. In the meantime, the gauge observations may experience large uncertainties and may result in the dry bias when estimating snowfall. Hence, the large differences between global reanalyses and CPCUGA over these regions during winter may be equally attributed to the observational uncertainties in CPCUGA and the modeling deficiencies of the reanalyses. For SGP and SE regions, the RDP distributions and values (Table 3) vary significantly from season to season, indicating the differences in reanalyses are perhaps due to the random errors. Additionally, all five of the global reanalyses seem to have systematic errors over the WC because their bias distributions, as well as the magnitudes of the RDP values, are very similar during the spring, fall, and winter seasons. The differences in distribution that occurred during summer could be due to the significantly lower precipitation amounts over WC region.

ERA-Interim, MERRA2, and CFSR show very similar systematic behaviors in the spatial distribution of RDPs during different seasons (Fig. 4) because they assimilate almost identical satellite radiance data as input into their models. Underestimations are also noticed in these three reanalyses over the central part of the country, where precipitation is related to atmosphere–land interactions that may be deficiently represented in the model. During summer, when convective precipitation events occur over the Great Plain regions, more severe underestimations are found in these three reanalyses, implying that the negative biases might be caused by the convective parameterization of the models. Besides assimilating
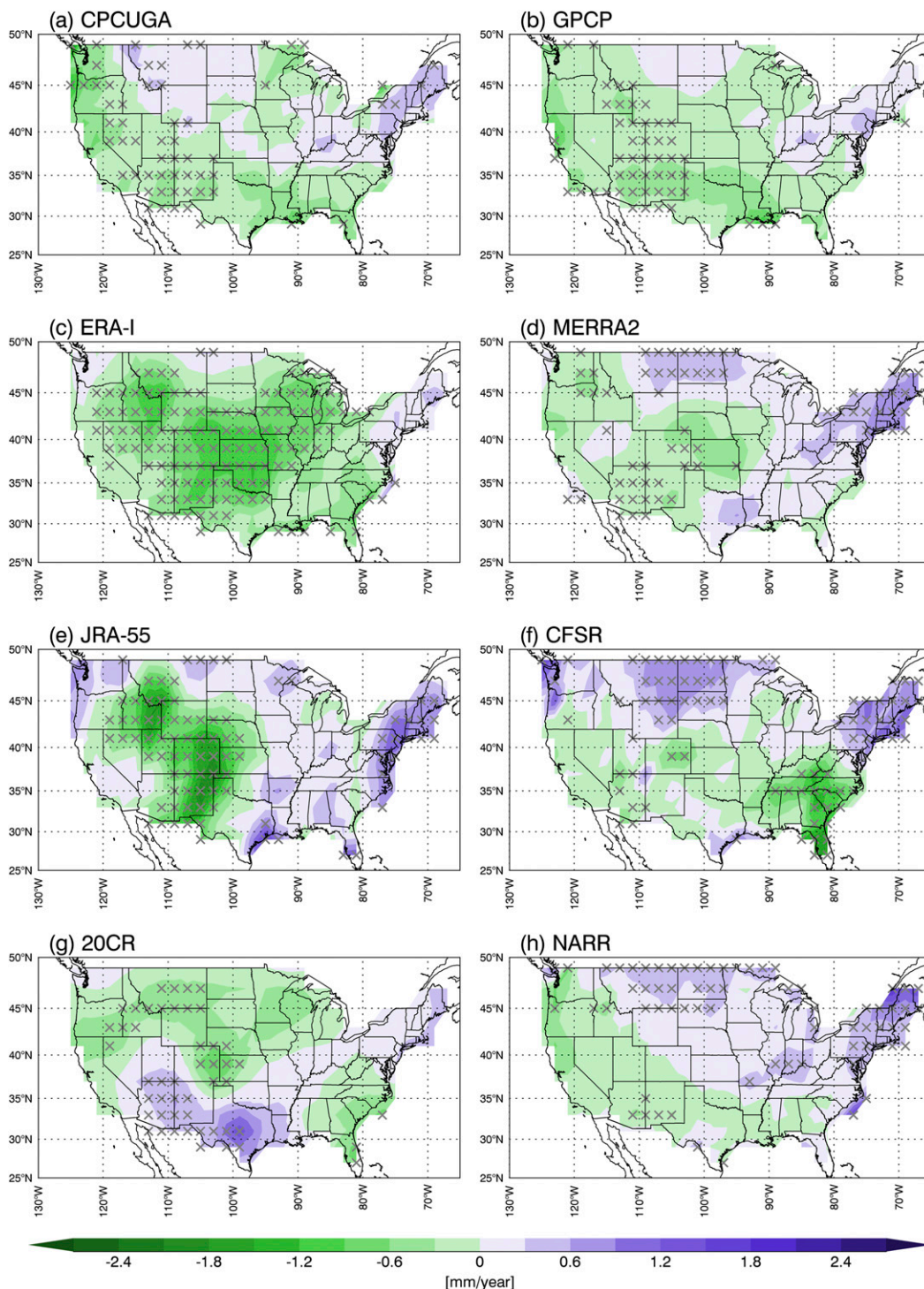
FIG. 8. Spatial distribution of monthly precipitation anomaly trend of CPCUGA, GPCP, and six reanalyses during the period 1980–2013. The gray crosses indicate the grid boxes with statistical significance at the 95% confidence level based on the Mann–Kendall test.

the satellite retrievals used in the ERA-Interim, the radiance data from the Japanese GMS and Multifunctional Transport Satellite (MTSAT) are reprocessed in

JRA-55, which is only done by JRA-55; in addition, no IR data were used in JRA-55 after 2003. Therefore, JRA-55 shows similar characteristics in RDP
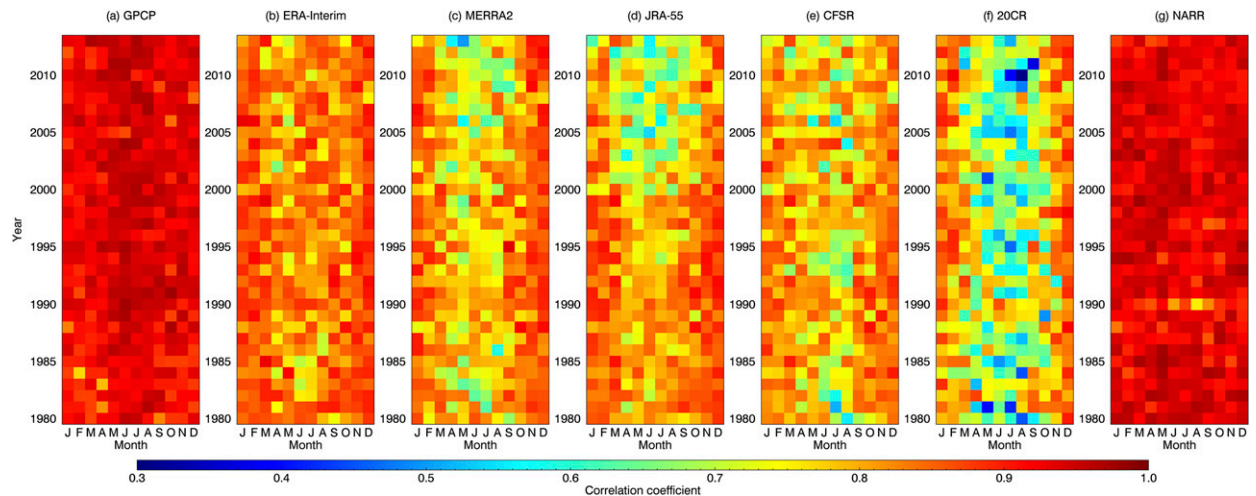
FIG. 9. Correlation coefficients between CPCUGA and GPCP and between CPCUGA and the reanalyses for each monthly precipitation value; the value calculated for each box is based on 260 grid boxes over the CONUS domain. The x axis represents the month and the y axis represents the year.

distribution but also shows differences over the central part of the country (Fig. 4) compared to three reanalyses discussed above. The convective scheme adopted by JRA-55, particularly the inclusion of the DCAPE convection-triggering mechanism [CFSR and JRA-55 both use Arakawa and Schubert (1974) convective scheme], seems to produce more precipitation, as it overestimates the precipitation over the Great Plains during spring and summer.

Previous studies (Zhang et al. 2012; Rienecker et al. 2011; Robertson et al. 2011; Bosilovich et al. 2015) have shown that precipitation in global reanalysis datasets is very sensitive to the observation system. For example, with the introduction of SSM/I in late 1987 and the Advanced Microwave Sounding Unit-A (AMSU-A) series in late 1998, series of jumps or shifts in trend were found in MERRA and ERA-Interim global precipitation (Rienecker et al. 2011). In this study, however, it is noteworthy that although the interannual variability seems to be represented well by all reanalyses, unreasonable linear and spatial trends are generated by these reanalyses. For example, ERA-Interim shows a significant decreasing linear trend of -4.53 mm yr^{-1} in precipitation during the study period. Simmons et al. (2010) found that this trend is more related to a declining shift that starts in the early 1990s and considered that it may be related to the prescribed SSTs used in ERA-Interim. Therefore, caution should be taken when employing reanalyzed precipitation in trend studies. The biases existing in reanalyses should also be considered when using them for different applications, for example, consistent positive biases are found in MERRA2,

JRA-55, CFSR, and 20CRv2c, while a consistent negative bias is found in NARR. To further investigate the influence of changes in observation data and how these changes may affect the quality of reanalyzed precipitation, correlation coefficients and RMSEs are computed between CPCUGA and GPCP and between CPCUGA and reanalyses for the monthly precipitation values at each of the 260 grid boxes over the CONUS domain. These results are presented in Figs. 9 and 10, respectively. ERA-Interim and CPCUGA are in good agreement throughout the entire study period, except for several months that have comparably lower correlations (~0.75) during the pre-SSM/I period. MERRA2, JRA-55, and CFSR compare reasonably well with CPCUGA, but their performance appears to drop off after 2005 in MERRA2 and after mid-2000 in JRA-55. In global reanalyses, satellite radiance data are used to determine the humidity information as input into the models (Dee et al. 2011; Koster et al. 2016), where humidity is usually calculated based on empirical statistical methods from satellite retrievals. These empirical relationships are based on observational studies, but, because of some changes in atmospheric moisture structure with time, the humidity profiles in recent years may not be accurately characterized by these empirical approaches. This may introduce errors into precipitation output and lead to the decreasing correlations with time found in MERRA2 and JRA-55. Additionally, the drop-off in correlation values in JRA-55 may also be due to the atmospheric motion vector (AMV) data from geostationary and polar-orbiting satellites not being reprocessed after
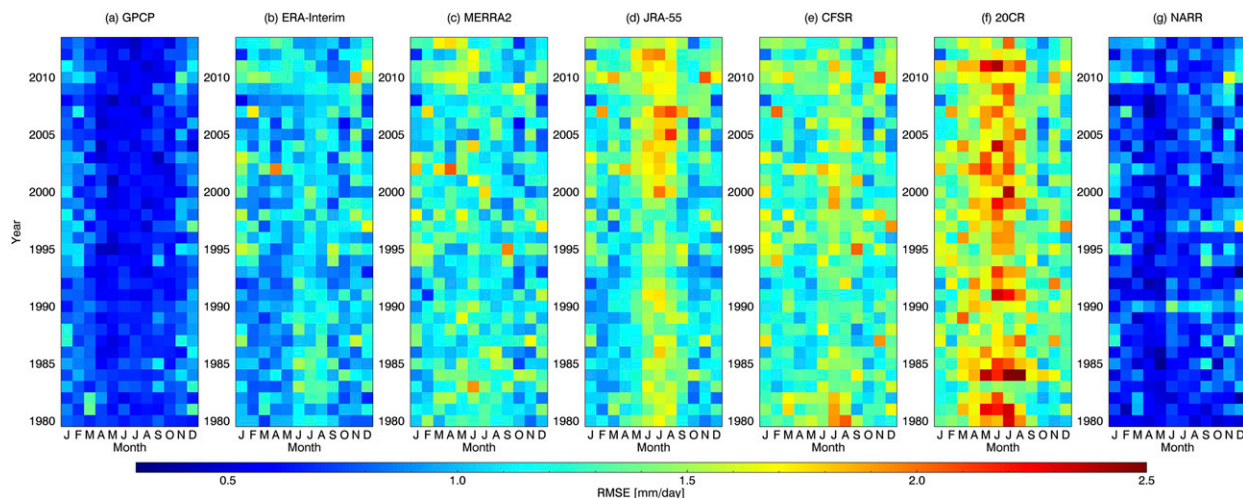
FIG. 10. As in Fig. 9, but for RMSE.

June 2004 and no IR radiance data being used since 2003 (Kobayashi et al. 2015). Zhang et al. (2012) found that CFSR has a sudden change in precipitation in 1998 resulting from the inclusion of ATOVS data. However, in this study, the correlations and RMSEs of CFSR are relatively consistent over time. Again, very strong correlations (~0.95) and low RMSEs are found in NARR during the study period owing to the assimilation of gauge observations, though relatively lower correlation coefficients are found from March to October 1990. Note that during the spring and summer seasons, five global reanalyses have higher RMSEs and are less correlated with CPCUGA, which could be associated with the systematic errors of the assimilation models, which support the results in Ashouri et al. (2016) that MERRA has issues in reproducing extreme precipitation over the Great Plains and in Prakash et al. (2015) that larger bias and RMSEs are found in reanalyses over the North American monsoon region. GPCP shows consistently high correlation coefficients with CPCUGA (~0.95), and similar to ERA-Interim, several months with slightly lower correlations around 0.8 are found before the SSM/I period. Contrary to the behavior of global reanalyses, GPCP has higher correlations and lower RMSEs during the spring and summer months.

20CRv2c only assimilates SLP and SST observations, and thus it is resistant to the introductions of new observing systems (Lee and Biasutti 2014). Therefore, 20CRv2c has less in common with other reanalyses' precipitation fields during the comparisons. Nevertheless, the biases in precipitation generated by 20CRv2c are more significant than in the comprehensive reanalyses, which produce the highest RDPs and RMSEs throughout the year, the lowest spatial correlation coefficients (Fig. 5), and some unrealistic interannual variations (Fig. 7). This inaccuracy in representing precipitation in 20CRv2c could be because SST and SLP data are less related to atmospheric moisture and thus the model cannot reproduce the physical and dynamical processes when generating precipitation analysis. Note that despite a dense observational network and a complete sea level pressure record through the satellite era over the United States (Lee and Biasutti 2014), the performance of 20CRv2c, when compared with two reference data, is still the worst among the reanalysis datasets in this study. This is not unexpected due to the simplicity of the data ingested—a sacrifice made for a longer data record.

NARR performs better in reproducing precipitation than global reanalyses because it indirectly uses rain gauge analysis. Negative biases are found in NARR over the most of the CONUS domain, which may be related to a model deficiency and errors in its objective analysis technique, and these should be addressed in future versions. Assimilation of precipitation observations in reanalyses can help produce more accurate precipitation analysis fields and improve the quality of output variables from land surface analysis, because model-generated precipitation is usually used as forcing data for the land surface model in reanalyses, such as in JRA-55.

6. Conclusions

This study evaluates the performance of precipitation data from six recently developed reanalysis products with gridded gauge data CPCUGA and satellite–gauge combined GPCP product over the CONUS from January 1980 through December 2013. Based on the results

from 34-yr comparisons and trend analysis, we summarize the following conclusions:

1) Strong agreements are found between two reference datasets, but the overall precipitation derived from GPCP is around 8% higher than CPCUGA—this bias should be taken into account when using GPCP to validate the global precipitation from climate models. In addition, GPCP estimates may be less trustworthy over the orographic terrain. The precipitation generated by four reanalyses that assimilate satellite radiance observations tend to be more similar to GPCP-derived precipitation, which is not unexpected because they use similar satellite data.

2) All of the reanalyses are able to depict reasonable spatial patterns and amounts of precipitation over the CONUS, especially for the northwestern part of the country. However, global reanalyses generally overestimate the precipitation over the mountainous regions throughout the year and underestimate the precipitation over the Great Plains during summer as well as over the north-central and northeastern regions during winter.

3) For interannual precipitation, MERRA2, JRA-55, CFSR, and 20CRv2c have positive biases while NARR has negative bias throughout the study period. Some of the interannual variability of CPCUGA precipitation is well represented by the six reanalyses. The annual accumulated precipitation over the CONUS has a decreasing trend of $-1.38\,\mathrm{mm\,yr^{-1}}$ during the study period based on CPCUGA data. Determined by the observed precipitation, the north-central and northeastern parts of the country show positive trends, while most other regions show negative trends, with statistically significant negative trends over the mountainous regions. However, none of the reanalyses generate reasonable linear or spatial trends as found in the two reference datasets.

4) For users of reanalysis products, we conclude that ERA-Interim and NARR are comparatively better at representing the precipitation over the CONUS as indicated by their correlation coefficients and standard deviations against both CPCUGA and GPCP estimates. Even though a decreasing trend exists in ERA-Interim, it is still the second-most consistent reanalysis product when compared against the CPCUGA.

Overall, although reanalyses can provide realistic precipitation analysis, caution should still be taken when using reanalyzed precipitation data for climate studies. For instance, errors may exist in model land–atmosphere interactions and convective and snowfall parameterizations. Even though changes in the observing system seem to have little influence on the continuity and quality of precipitation over the CONUS, they may still cause inhomogeneities in reanalyzed climate over parts of the world where radiosonde data are less available and the modeled precipitation is highly dependent upon satellite observations, such as over oceans and Africa. Furthermore, the general type and quality of assimilated data will largely affect the performance of reanalyses. The results presented in this study provide useful information on the limitations and strengths of each reanalysis dataset and suggest substantial efforts are necessary to further improve the reanalysis precipitation estimates in future versions.

REFERENCES

Adler, R. F., and Coauthors, 2003: The version-2 Global Precipitation Climatology Project (GPCP) Monthly Precipitation Analysis (1979–present). *J. Hydrometeor.*, **4**, 1147–1167, doi:10.1175/1525-7541(2003)004<1147:TVGPCP>2.0.CO;2.

Alpert, J., M. Kanamitsu, P. Caplan, J. Sela, and G. White, 1988: Mountain induced gravity wave drag parameterization in the NMC medium-range forecast model. Preprints, *Eighth Conf. on Numerical Weather Prediction*, Baltimore, MD, Amer. Meteor. Soc., 726–733.

Arakawa, A., and W. H. Schubert, 1974: Interaction of a cumulus cloud ensemble with the large-scale environment, Part I. *J. Atmos. Sci.*, **31**, 674–701, doi:10.1175/1520-0469(1974)031<0674:IOACCE>2.0.CO;2.

Arkin, P. A., and B. N. Meisner, 1987: The relationship between large-scale convective rainfall and cold cloud over the Western Hemisphere during 1982–84. *Mon. Wea. Rev.*, **115**, 51–74, doi:10.1175/1520-0493(1987)115<0051:TRBLSC>2.0.CO;2.

Ashouri, H., S. Sorooshian, K. L. Hsu, M. G. Bosilovich, J. Lee, M. F. Wehner, and A. Collow, 2016: Evaluation of NASA's MERRA precipitation product in reproducing the observed trend and distribution of extreme precipitation events in the United States. *J. Hydrometeor.*, **17**, 693–711, doi:10.1175/JHM-D-15-0097.1.

Betts, A. K., 1986: A new convective adjustment scheme. Part I: Observational and theoretical basis. *Quart. J. Roy. Meteor. Soc.*, **112**, 677–691, doi:10.1002/qj.49711247307.

Blacutt, L. A., D. L. Herdies, L. G. G. De Gonçalves, D. A. Vila, and M. Andrade, 2015: Precipitation comparison for the CFSR, MERRA, TRMM3B42 and Combined Scheme datasets in Bolivia. *Atmos. Res.*, **163**, 117–131, doi:10.1016/j.atmosres.2015.02.002.

Bosilovich, M. G., 2013: Regional climate and variability of NASA MERRA and recent reanalyses: U.S. summertime precipitation and temperature. *J. Appl. Meteor. Climatol.*, **52**, 1939–1951, doi:10.1175/JAMC-D-12-0291.1.

——, J. Chen, F. R. Robertson, and R. F. Adler, 2008: Evaluation of global precipitation in reanalyses. *J. Appl. Meteor. Climatol.*, **47**, 2279–2299, doi:10.1175/2008JAMC1921.1.

——, R. Lucchesi, and M. Suarez, 2015: MERRA-2: File specification. GMAO Office Note 9 (version 1.0), 73 pp. [Available online at https://ntrs.nasa.gov/archive/nasa/casi.ntrs.nasa.gov/20150019760.pdf.]

Bukovsky, M. S., and D. J. Karoly, 2007: A brief evaluation of precipitation from the North American Regional Reanalysis. *J. Hydrometeor.*, **8**, 837–846, doi:10.1175/JHM595.1.

Chen, M., W. Shi, P. Xie, V. Silva, V. E. Kousky, R. W. Higgins, and J. E. Janowiak, 2008a: Assessing objective techniques for gauge-based analyses of global daily precipitation. *J. Geophys. Res.*, **113**, D04110, doi:10.1029/2007JD009132.

——, P. Xie, and W. Shi, 2008b: CPC Unified Gauge-Based Analysis of global daily precipitation. *24th Conf. on Hydrology*, Atlanta, GA, Amer. Meteor. Soc., 2.3A. [Available online at https://ams.confex.com/ams/90annual/techprogram/paper_163676.htm.]

Compo, G. P., and Coauthors, 2011: The Twentieth Century Reanalysis Project. *Quart. J. Roy. Meteor. Soc.*, **137**, 1–28, doi:10.1002/qj.776.

Daly, C., R. P. Neilson, and D. L. Phillips, 1994: A statistical–topographic model for mapping climatological precipitation over mountainous terrain. *J. Appl. Meteor.*, **33**, 140–158, doi:10.1175/1520-0450(1994)033<0140:ASTMFM>2.0.CO;2.

Dee, D., and Coauthors, 2011: The ERA-Interim reanalysis: Configuration and performance of the data assimilation system. *Quart. J. Roy. Meteor. Soc.*, **137**, 553–597, doi:10.1002/qj.828.

Dolinar, E. K., X. Dong, and B. Xi, 2016: Evaluation and intercomparison of clouds, precipitation, and radiation budgets in recent reanalyses using satellite-surface observations. *Climate Dyn.*, **46**, 2123–2144, doi:10.1007/s00382-015-2693-z.

Fensholt, R., and K. Rasmussen, 2011: Analysis of trends in the Sahelian 'rain-use efficiency' using GIMMS NDVI, RFE and GPCP rainfall data. *Remote Sens. Environ.*, **115**, 438–451, doi:10.1016/j.rse.2010.09.014.

Fisher, R. A., 1915: Frequency distribution of the values of the correlation coefficient in samples from an indefinitely large population. *Biometrika*, **10**, 507–521, doi:10.2307/2331838.

Grody, N. C., 1991: Classification of snow cover and precipitation using the Special Sensor Microwave/Imager (SSM/I). *J. Geophys. Res.*, **96**, 7423–7435, doi:10.1029/91JD00045.

Gu, G., R. F. Adler, G. J. Huffman, and S. Curtis, 2007: Tropical rainfall variability on interannual-to-interdecadal/longer-time

scales derived from the GPCP monthly product. *J. Climate*, **20**, 4033–4046, doi:10.1175/JCLI4227.1.

Hatzianastassiou, N., C. D. Papadimas, C. J. Lolis, A. Bartzokas, V. Levizzani, J. D. Pnevmatikos, and B. D. Katsoulis, 2016: Spatial and temporal variability of precipitation over the Mediterranean Basin based on 32-year satellite Global Precipitation Climatology Project data, part I: Evaluation and climatological patterns. *Int. J. Climatol.*, **36**, 4741–4754, doi:10.1002/joc.4666.

Hong, S. Y., and H. L. Pan, 1998: Convective trigger function for a mass-flux cumulus parameterization scheme. *Mon. Wea. Rev.*, **126**, 2599–2620, doi:10.1175/1520-0493(1998)126<2599:CTFFAM>2.0.CO;2.

Huffman, G. J., and D. T. Bolvin, 2013: GPCP version 2.2 SG combined precipitation data set documentation. NASA GSFC Doc., 46 pp. [Available online at ftp://precip.gsfc.nasa.gov/pub/gpcp-v2.2/doc/V2_doc.pdf.]

——, R. F. Adler, D. T. Bolvin, and G. Gu, 2009: Improving the global precipitation record: GPCP version 2.1. *Geophys. Res. Lett.*, **36**, L17808, doi:10.1029/2009GL040000.

Janjić, Z. I., 1995: A note on the performance of the multiply-upstream semi-Lagrangian advection schemes for one-dimensional nonlinear momentum conservation equation. *Meteor. Atmos. Phys.*, **55**, 1–16, doi:10.1007/BF01029598.

Kendall, M., 1975: *Multivariate Analysis.* Charles Griffin, 218 pp.

Kim, Y. J., and A. Arakawa, 1995: Improvement of orographic gravity wave parameterization using a mesoscale gravity wave model. *J. Atmos. Sci.*, **52**, 1875–1902, doi:10.1175/1520-0469(1995)052<1875:IOOGWP>2.0.CO;2.

Kishore, P., S. Jyoth, G. Basha, S. V. B. Rao, M. Rajeevan, I. Velicogna, and T. C. Sutterley, 2016: Precipitation climatology over India: Validation with observations and reanalysis datasets and spatial trends. *Climate Dyn.*, **46**, 541–556, doi:10.1007/s00382-015-2597-y.

Kobayashi, S., and Coauthors, 2015: The JRA-55 reanalysis: General specifications and basic characteristics. *J. Meteor. Soc. Japan*, **93**, 5–48, doi:10.2151/jmsj.2015-001.

Koster, R. D., and Coauthors, 2016: MERRA-2 input observations: Summary and assessment. NASA/TM-2016-104606/Vol. 46, 51 pp. [Available online at https://ntrs.nasa.gov/archive/nasa/casi.ntrs.nasa.gov/20160014544.pdf.]

Lee, D. E., and M. Biasutti, 2014: Climatology and variability of precipitation in the Twentieth Century Reanalysis. *J. Climate*, **27**, 5964–5981, doi:10.1175/JCLI-D-13-00630.1.

Lopez, P., and E. Moreau, 2005: A convection scheme for data assimilation: Description and initial tests. *Quart. J. Roy. Meteor. Soc.*, **131**, 409–436, doi:10.1256/qj.04.69.

Ma, L., T. Zhang, O. W. Frauenfeld, B. Ye, D. Yang, and D. Qin, 2009: Evaluation of precipitation from the ERA-40, NCEP-1, and NCEP-2 reanalyses and CMAP-1, CMAP-2, and GPCP-2 with ground-based measurements in China. *J. Geophys. Res.*, **114**, D09105, doi:10.1029/2008JD011178.

Mann, H. B., 1945: Nonparametric tests against trend. *Econometrica*, **13**, 245–259, doi:10.2307/1907187.

McPhee, J., and S. A. Margulis, 2005: Validation and error characterization of the GPCP-1DD precipitation product over the contiguous United States. *J. Hydrometeor.*, **6**, 441–459, doi:10.1175/JHM429.1.

Mesinger, F., and Coauthors, 2006: North American Regional Reanalysis. *Bull. Amer. Meteor. Soc.*, **87**, 343–360, doi:10.1175/BAMS-87-3-343.

Molod, A. M., L. L. Takacs, M. Suarez, and J. Bacmeister, 2015: Development of the GEOS-5 atmospheric general circulation

model: Evolution from MERRA to MERRA2. *Geosci. Model Dev.*, **8**, 1339–1356, doi:10.5194/gmd-8-1339-2015.

Moorthi, S., and M. J. Suarez, 1992: Relaxed Arakawa–Schubert: A parameterization of moist convection for general circulation models. *Mon. Wea. Rev.*, **120**, 978–1002, doi:10.1175/1520-0493(1992)120<0978:RASAPO>2.0.CO;2.

Nakagawa, M., and A. Shimpo, 2004: Development of a cumulus parameterization scheme for the operational global model at JMA. RSMC Tokyo-Typhoon Center Tech. Review 7, Japan Meteorological Agency, 10–15. [Available online at http://www.jma.go.jp/jma/jma-eng/jma-center/rsmc-hp-pub-eg/techrev/text7-2.pdf.]

Nijssen, B., G. M. O'Donnell, D. P. Lettenmaier, D. Lohmann, and E. F. Wood, 2001: Predicting the discharge of global rivers. *J. Climate*, **14**, 3307–3323, doi:10.1175/1520-0442(2001)014<3307:PTDOGR>2.0.CO;2.

Onogi, K., and Coauthors, 2007: The JRA-25 reanalysis. *J. Meteor. Soc. Japan*, **85**, 369–432, doi:10.2151/jmsj.85.369.

Pan, H. L., and W. S. Wu, 1995: Implementing a mass flux convective parameterization package for the NMC medium range forecast model. NMC Office Note 409, NOAA, 43 pp. [Available online at http://www2.mmm.ucar.edu/wrf/users/phys_refs/CU_PHYS/Old_SAS.pdf.]

Prakash, S., R. M. Gairola, and A. K. Mitra, 2015: Comparison of large-scale global land precipitation from multisatellite and reanalysis products with gauge-based GPCC data sets. *Theor. Appl. Climatol.*, **121**, 303–317, doi:10.1007/s00704-014-1245-5.

Randall, D. A., and D. M. Pan, 1993: Implementation of the Arakawa–Schubert cumulus parameterization with a prognostic closure. *The Representation of Cumulus Convection in Numerical Models, Meteor. Monogr.*, No. 46, Amer. Meteor. Soc., 137–144.

Rienecker, M. M., and Coauthors, 2008: The GEOS-5 Data Assimilation System—Documentation of versions 5.0.1, 5.1.0, and 5.2.0. Tech. Memo. NASA/TM-2008-104606, Vol. 27, 97 pp. [Available online at http://gmao.gsfc.nasa.gov/pubs/docs/Rienecker369.pdf.]

——, and Coauthors, 2011: MERRA: NASA's Modern-Era Retrospective Analysis for Research and Applications. *J. Climate*, **24**, 3624–3648, doi:10.1175/JCLI-D-11-00015.1.

Robertson, F. R., M. G. Bosilovich, J. Chen, and T. L. Miller, 2011: The effect of satellite observing system changes on MERRA water and energy fluxes. *J. Climate*, **24**, 5197–5217, doi:10.1175/2011JCLI4227.1.

Saha, S., and Coauthors, 2010: The NCEP Climate Forecast System Reanalysis. *Bull. Amer. Meteor. Soc.*, **91**, 1015–1057, doi:10.1175/2010BAMS3001.1.

Simmons, A., K. M. Willett, P. D. Jones, P. W. Thorne, and D. P. Dee, 2010: Low-frequency variations in surface atmospheric humidity, temperature, and precipitation: Inferences from reanalyses and monthly gridded observational data sets. *J. Geophys. Res.*, **115**, D01110, doi:10.1029/2009JD012442.

Stanfield, R., X. Dong, B. Xi, A. Del Genio, P. Minni, D. Doelling, and N. Loeb, 2015: Assessment of NASA GISS CMIP5 and post-CMIP5 simulated clouds and TOA radiation budgets using satellite observations. Part II: TOA radiation budgets and cloud radiative forcings. *J. Climate*, **28**, 1842–1864, doi:10.1175/JCLI-D-14-00249.1.

Sundqvist, H., 1978: A parameterization scheme for non-convective condensation including prediction of cloud water content. *Quart. J. Roy. Meteor. Soc.*, **104**, 677–690, doi:10.1002/qj.49710444110.

——, E. Berge, and J. E. Kristjánsson, 1989: Condensation and cloud parameterization studies with a mesoscale numerical weather prediction model. *Mon. Wea. Rev.*, **117**, 1641–1657, doi:10.1175/1520-0493(1989)117<1641:CACPSW>2.0.CO;2.

Susskind, J., and J. Pfaendtner, 1989: Impact of interactive physical retrievals on NWP. *Report on the Joint ECMWF/EUMETSAT Workshop on the Use of Satellite Data in Operational Weather Prediction: 1989–1993*, T. Hollingsworth, Ed., Vol. 1, ECMWF, 245–270.

——, P. Piraino, L. Rokke, T. Iredell, and A. Mehta, 1997: Characteristics of the TOVS Pathfinder Path A dataset. *Bull. Amer. Meteor. Soc.*, **78**, 1449–1472, doi:10.1175/1520-0477(1997)078<1449:COTTPP>2.0.CO;2.

Tiedtke, M., 1983: The sensitivity of the time-mean large-scale flow to cumulus convection in the ECMWF model. *Proc. Workshop on Convection in Large-Scale Numerical Models*, Reading, United Kingdom, ECMWF, 297–316. [Available online at https://www.ecmwf.int/en/elibrary/12733-sensitivity-time-mean-large-scale-flow-cumulus-convection-ecmwf-model.]

Wang, A., and X. Zeng, 2012: Evaluation of multireanalysis products with in situ observations over the Tibetan Plateau. *J. Geophys. Res.*, **117**, D05102, doi:10.1029/2011JD016553.

Whitaker, J. S., and T. M. Hamill, 2002: Ensemble data assimilation without perturbed observations. *Mon. Wea. Rev.*, **130**, 1913–1924, doi:10.1175/1520-0493(2002)130<1913:EDAWPO>2.0.CO;2.

Wilheit, T., A. Chang, and L. Chiu, 1991: Retrieval of monthly rainfall indices from microwave radiometric measurements using probability distribution functions. *J. Atmos. Oceanic Technol.*, **8**, 118–136, doi:10.1175/1520-0426(1991)008<0118:ROMRIF>2.0.CO;2.

Xie, P., and P. A. Arkin, 1998: Global monthly precipitation estimates from satellite-observed outgoing longwave radiation. *J. Climate*, **11**, 137–164, doi:10.1175/1520-0442(1998)011<0137:GMPEFS>2.0.CO;2.

——, J. E. Janowiak, P. A. Arkin, R. F. Adler, A. Gruber, R. Ferraro, G. J. Huffman, and S. Curtis, 2003: GPCP pentad precipitation analyses: An experimental dataset based on gauge observations and satellite estimates. *J. Climate*, **16**, 2197–2214, doi:10.1175/2769.1.

——, M. Chen, S. Yang, A. Yatagai, T. Hayasaka, Y. Fukushima, and C. Liu, 2007: A gauge-based analysis of daily precipitation over East Asia. *J. Hydrometeor.*, **8**, 607–626, doi:10.1175/JHM583.1.

Xie, S. C., and M. H. Zhang, 2000: Impact of the convective triggering function on single-column model simulations. *J. Geophys. Res.*, **105**, 14 983–14 996, doi:10.1029/2000JD900170.

Zhang, L., A. Kumar, and W. Wang, 2012: Influence of changes in observations on precipitation: A case study for the Climate Forecast System Reanalysis (CFSR). *J. Geophys. Res.*, **117**, D08105, doi:10.1029/2011JD017347.

Zhao, Q. Y., and F. H. Carr, 1997: A prognostic cloud scheme for operational NWP models. *Mon. Wea. Rev.*, **125**, 1931–1953, doi:10.1175/1520-0493(1997)125<1931:APCSFO>2.0.CO;2.